THE JOURNAL OF BIOLOGICAL CHEMISTRY VOL. 287, NO. 33, pp. 27823–27833, August 10, 2012

Conserved Chloroplast Open-reading Frame *ycf54* Is Required for Activity of the Magnesium Protoporphyrin Monomethylester Oxidative Cyclase in *Synechocystis* PCC 6803[S]

Received for publication, February 12, 2012, and in revised form, June 17, 2012 Published, JBC Papers in Press, June 18, 2012, DOI 10.1074/jbc.M112.352526

Sarah Hollingshead[‡1] **Jana Kopečná**[§¶], **Philip J. Jackson**[‡‖2] **Daniel P. Canniffe**[‡2], **Paul A. Davison**[‡3], **Mark J. Dickman**[‖2], **Roman Sobotka**[§¶4], **and C. Neil Hunter**[‡2]

From the [‡]*Department of Molecular Biology and Biotechnology, University of Sheffield, Firth Court, Western Bank, Sheffield S10 2TN, United Kingdom,* [§]*Institute of Microbiology, Department of Phototrophic Microorganisms, Opatovicky mlyn, 379 81 Trebon, Czech Republic,* [¶]*Faculty of Sciences, University of South Bohemia, Branisovska 31, 370 05 Ceske Budejovice, Czech Republic, and* [‖]*ChELSI Institute, Department of Chemical and Biological Engineering, University of Sheffield, Mappin Street, Sheffield, S1 3JD, United Kingdom*

Background: The cyclase step in chlorophyll biosynthesis remains uncharacterized.
Results: Ycf54 forms a complex with other oxidative cyclase components, and a *ycf54* mutant accumulates the cyclase substrate.
Conclusion: Ycf54 is essential for cyclase function.
Significance: Identification of all of the components of chlorophyll biosynthesis is a step closer.

The cyclase step in chlorophyll (Chl) biosynthesis has not been characterized biochemically, although there are some plausible candidates for cyclase subunits. Two of these, Sll1214 and Sll1874 from the cyanobacterium *Synechocystis* 6803, were FLAG-tagged *in vivo* and used as bait in separate pulldown experiments. Mass spectrometry identified Ycf54 as an interaction partner in each case, and this interaction was confirmed by a reciprocal pulldown using FLAG-tagged Ycf54 as bait. Inactivation of the *ycf54* gene (*slr1780*) in *Synechocystis* 6803 resulted in a strain that exhibited significantly reduced Chl levels. A detailed analysis of Chl precursors in the *ycf54* mutant revealed accumulation of very high levels of Mg-protoporphyrin IX methyl ester and only traces of protochlorophyllide, the product of the cyclase, were detected. Western blotting demonstrated that levels of the cyclase component Sll1214 and the Chl biosynthesis enzymes Mg-protoporphyrin IX methyltransferase and protochlorophyllide reductase are significantly impaired in the *ycf54* mutant. Ycf54 is, therefore, essential for the activity and stability of the oxidative cyclase. We discuss a possible role of Ycf54 as an auxiliary factor essential for the assembly of a cyclase complex or even a large multienzyme catalytic center.

Chlorophylls (Chls)[5] are key cofactors of the photosynthetic apparatus, and their biosynthesis results in the formation of the most abundant natural pigments on Earth. Chl is structurally distinguished from other tetrapyrroles such as hemes, bilins, or corrins, by a centrally chelated magnesium atom and by the presence of an isocyclic "fifth" ring. In plants, algae, and cyanobacteria the synthesis of Chl, heme, and bilins shares the same pathway up until protoporphyrin IX (P_{IX}), which is used as a substrate for two different chelatases. Whereas insertion of Fe^{2+} results in heme, insertion of Mg^{2+} by magnesium chelatase leads to Mg-protoporphyrin IX (MgP), the first intermediate on the Chl branch. MgP is converted to Mg-protoporphyrin IX methylester (MgPME) by Mg-protoporphyrin methyltransferase. The isocyclic ring is made in the following step by the oxidative MgPME cyclase (EC 1.14.13.81, hereafter MgPME cyclase), which results in the Chl *a* precursor protochlorophyllide (PChlide). Conversion of PChlide to chlorophyllide (Chlide) is catalyzed by PChlide oxidoreductase, and Chl *a* is finally completed by the addition of a polyisoprene tail to Chlide by the Chl-synthase (for review, see Ref. 1).

Although cyclase activity was assayed many years ago using cucumber chloroplasts (2–4), wheat etioplasts (5) and cell extracts from *Chlamydomonas reinhardtii* and *Synechocystis* PCC 6803 (6), the enzyme itself remains enigmatic. Formation of the isocyclic ring is proposed to be a complex enzymatic reaction that consists of three sequential steps: (*a*) hydroxylation of the ring C to methylpropionate, (*b*) oxidation to ketopropionate, (*c*) ligation of an activated methylene group to the γ-meso carbon of the porphyrin ring (7, 8); see supplemental Fig. S1 for a series of reactions proposed for the cyclase step. Biochemical characterization also provided evidence for the incorporation of atmospheric oxygen into synthetized PChlide in plants (9), which implies that the oxidative cyclase differs structurally and mechanistically from the anaerobic MgPME cyclase identified from analysis of *bchE* mutants of *Rhodobacter capsulatus* and *Rhodobacter sphaeroides* (10–12). In the anaerobic cyclase the 13^1-oxo group of bacteriochlorophyll is derived

[S] This article contains supplemental Figs. S1–S5.
[1] Supported by a doctoral studentship from the University of Sheffield.
[2] Supported by a grant from the Biotechnology and Biological Sciences Research Council (United Kingdom).
[3] Supported by postdoctoral funds from the University of Sheffield.
[4] Supported by the Grant Agency of the Czech Republic (projects P501/10/1000) and by projects Algatech (CZ.1.05/2.1.00/03.0110) and RVO61388971. To whom correspondence should be addressed: Institute of Microbiology, Dept. of Phototrophic Microorganisms, Opatovicky mlyn, 379 81 Trebon, Czech Republic. Tel.: 420-384-340434; Fax: 420-384-340415; E-mail sobotka@alga.cz.
[5] The abbreviations used are: Chl, chlorophyll; Chlide, chlorophyllide; PChlide, protochlorophyllide; MgP, Mg protoporphyrin; MgPME, Mg-protoporphyrin monomethyl ester; P_{IX}, protoporphyrin IX.

from water (13), whereas in aerobic phototrophs such as *Roseobacter denitrificans* this group arises from molecular oxygen (14).

Partial purification of oxidative cyclase from chloroplasts and cyanobacteria suggested that this enzyme requires several proteins (subunits) for activity (6, 15). The only known candidate for a catalytic cyclase subunit was identified by mutational analysis of the photosynthetic bacterium *Rubrivivax gelatinosus.* Although this bacterium also has a BchE homolog functional under anaerobic conditions, inactivation of the *acsF* gene resulted in accumulation of MgPME under aerobic conditions. Thus, *R. gelatinosus* possesses two unrelated MgPME cyclases, one oxygen-dependent and one oxygen-independent (16, 17). AcsF homologs have since been identified in many photosynthetic eukaryotes including *C. reinhardtii* (18), *Arabidopsis thaliana* (19), and barley (15). Two *acsF*-like genes, *sll1214* and *sll1874*, have been identified in *Synechocystis* PCC 6803 (hereafter *Synechocystis*) (20); Sll1214 is essential for growth under aerobic conditions (20) and, to a certain extent, micro-oxic conditions (21), whereas Sll1874 was found to be essential for growth in micro-oxic conditions (20, 21).

In this work we performed *in vivo* FLAG pulldown experiments using *Synechocystis* strains transformed with genes encoding either the FLAG-Sll1214 or FLAG-Sll1874 protein. Using mass spectrometry, we identified a Ycf54-like protein (Ycf54) as a putative assembly factor or subunit of the MgPME cyclase that interacts with both Sll1214 and Sll1874. This interaction was confirmed by a "reciprocal" co-purification of FLAG-Ycf54 together with Sll1214. Inactivation of the *ycf54* gene (*slr1780*) results in a significant reduction of cellular Chl and PChlide levels and the accumulation of MgPME. In addition this mutation strongly impairs accumulation of the Sll1214 cyclase component together with other enzymes in the Chl branch of tetrapyrrole pathway, particularly MgP methyltransferase and PChlide oxidoreductase. Thus, Ycf54 is essential for normal levels of MgPME cyclase activity and/or stability, suggesting that Ycf54 plays a critical role in assembly or function of the cyclase complex.

EXPERIMENTAL PROCEDURES

Growth Conditions—The *Synechocystis ycf54* strain and the control wild-type (WT) strain were grown photomixotrophically in a rotary shaker under low light conditions (3 μmol of photons m^{-2} s^{-1}) at 30 °C in liquid BG-11 medium (22) supplemented with 5 mM glucose.

Construction of FLAG-tagged Synechocystis Mutants—The plasmid pPD-FLAG was made to allow construction of *Synechocystis* strains expressing putative subunits of the cyclase with a 3×FLAG (hereafter FLAG) tag at the N terminus. pPD-FLAG contains the *Synechocystis psbAII* promoter, a sequence encoding the 3×FLAG tag and flanking sequences for homologous recombination that allows insertion of tagged constructs into the *Synechocystis* genome in place of the *psbAII* gene (see supplemental Fig. S2). The *sll1214*, *sll1874*, and *ycf54* genes were each subcloned into pPD-FLAG, and the resulting plasmids were transformed into the *Synechocystis* WT. Transformants were selected on a BG-11 agar plate containing 10 μg ml^{-1} neomycin and fully segregated by increasing the concentration of antibiotic to a final concentration of 80 μg ml^{-1}.

Preparation of Solubilized Membrane Fraction and Anti-FLAG Pulldown Assay—Synechocystis cells expressing genes for FLAG-tagged proteins were grown photoautotrophically to an OD_{750} of 0.5–0.7. Cells were pelleted, washed, and resuspended with buffer A (25 mM sodium phosphate, pH 7.4, 50 mM NaCl, 10 mM $MgCl_2$, 10% glycerol, EDTA-free protease inhibitor; Roche Applied Science). Cells were mixed in equal proportions with glass beads broken in a Mini-Beadbeater-16 (BioSpec), and the soluble proteins and membranes were separated by centrifugation (65,000 × *g*, 45 min). The membrane fraction was washed with, then resuspended in, buffer A and solubilized for 1 h at 4 °C with 1.5% dodecyl-β-maltoside (Glycon). Finally, insoluble contaminants were removed by centrifugation (65,000 × *g*, 25 min).

FLAG-Sll1214, FLAG-Sll1874, and FLAG-Ycf54 complexes were purified from soluble and membrane fractions by batch binding to anti-FLAG-M2-agarose (Sigma) for 1 h at room temperature. To remove contaminants the anti-FLAG-resin was washed with 100 resin volumes of buffer A containing 0.04% dodecyl-β-maltoside. The FLAG-tagged proteins were eluted with 2.5 resin volumes of buffer A containing 150 μg/ml 3×FLAG peptide (Sigma) and 0.04% dodecyl-β-maltoside.

Analysis by Nano-LC-MS/MS and Database Searching—The FLAG-eluted proteins were reduced in the presence of 100 mM triethylammonium bicarbonate, pH 8.5, 1% sodium dodecyl sulfate (SDS), and 50 mM dithiothreitol (all from Sigma) at 60 °C for 30 min. The proteins were then *S*-alkylated by incubation with 10 mM iodoacetamide (Sigma) at room temperature in the dark for 30 min. After a 10-fold dilution with 50 mM triethylammonium bicarbonate, the proteins were digested with 4 μg of trypsin (proteomics grade, Sigma) at 37 °C for 16 h followed by drying in a vacuum centrifuge. The tryptic peptides were redissolved in 0.2 ml of 10 mM potassium phosphate, pH 3, in 25% acetonitrile (loading buffer) with 7 μl of 0.5 M phosphoric acid added to acidify the samples and applied to homemade spin columns containing a 20-μl bed volume of Poros 20 SP cation exchange medium (Applied Biosystems). The columns were washed with 2× 0.1-ml loading buffer to remove SDS, and the tryptic peptides were eluted with 0.1 ml of loading buffer containing 0.5 M KCl. The samples were desalted using C_{18} reverse-phase Spin-Tips (Protea Biosciences) according to the manufacturer's protocol.

Tryptic peptides were separated using an UltiMate 3000 nanoflow liquid chromatography system (Dionex, Camberley, UK) with 5 mm × 300 μm (trapping) and 150 mm × 75 μm (analytical) PepMap C_{18} reverse-phase columns (Dionex). Linear gradient elution was from 97% solvent A (0.1% formic acid in 3% acetonitrile) to 35% solvent B (0.1% formic acid, 97% acetonitrile) at a flow rate of 300 nl/min for 40 min. On-line mass spectrometry was performed using a maXis UHR-TOF (Bruker Daltonics, Bremen, Germany) acquiring line spectra with automatic dependent MS/MS scans.

Peak lists for database searching in the form of Mascot Generic Files were created with DataAnalysis 4.0 software (Bruker). The Mascot Generic Files were submitted for database searching using Mascot Daemon v. 2.1.3 running with

Mascot Server v. 2.2.01 (Matrix Science, London, UK) against the *Synechocystis* complete proteome database (ExPASy). Search parameters were as follows: enzyme, trypsin; fixed modifications, carbamidomethyl (C); variable modifications, deamidation (NQ), oxidation (M); maximum missed cleavages, 1.

Inactivation of the ycf54 Gene—To prepare the *Synechocystis ycf54* strain, chromosomal DNA was isolated from a non-segregated *Synechocystis ycf54* mutant obtained as a generous gift from Prof. Teruo Ogawa (Nagoya University, Japan). The mutated allele of the *ycf54* is interrupted by an erythromycin resistance cassette inserted at nucleotide 129 of the *ycf54* gene. The chromosomal DNA was transformed into *Synechocystis* WT, and transformants were selected on BG-11 agar plates containing 10 μg of ml^{-1} erythromycin and then segregated under low light (3 μmol of photons m^{-2} s^{-1}) on 5 mM glucose and increasing concentrations of erythromycin to a final concentration of 80 μg ml^{-1}. The mutant is designated as *ycf54* in cases where it is partially segregated and *ycf54*$^{-}$ when it has been complemented with the FLAG-*ycf54* construct and full segregation was achieved.

Quantification of Chlorophyll and Chlorophyll Precursors— To measure Chl content per cell, pigments were extracted from cell pellets (5 ml, $OD_{750} \sim 0.4$) with an excess of 100% methanol, and the Chl content was measured spectrophotometrically (23). To compare the contents of all other abundant cellular pigments, the same methanol extract was immediately injected onto an HPLC machine (Agilent-1200), and the pigments were separated using a reverse phase column (Nova-Pak C18, 4 μm particle size, 3.9 × 150 mm; Waters) with 30% methanol in 1 M ammonium acetate, pH 6.0, and 40% acetone in methanol as solvents A and B, respectively. Pigments were eluted with a linear gradient of solvent B (45–100% in 18 min) followed by 100% of B at a flow rate of 1 ml min^{-1} at 40 °C. For quantitative determination of Chl precursors, 75 ml of culture at OD_{750} = 0.35–0.4 was filtered through a 4-μm cellulose filter to remove precipitated pigments in the growth medium and harvested. Pigments were extracted with an excess of 80% methanol, 20% water, 0.2% NH_4OH and measured as described previously (24), except in the present work the HPLC was equipped with two fluorescence detectors and a diode array detector. The first fluorescence detector was set to 440/670 nm (excitation/emission wavelengths) for 0–11 min, 440/640 nm for 11–14 min, and 400/630 nm for 14–25 min. The second fluorescence detector was set at 416/595 nm throughout the experiment.

Preparation of Antibodies—To prepare an antibody against the Ycf54 protein, the *ycf54* gene was amplified from *Synechocystis* genomic DNA and cloned into pGEX-4-T1 (GE Healthcare). The GST-Ycf54 gene fusion was overexpressed in *Escherichia coli* BL21 cells followed by purification on GST affinity resin, removal of the GST tag by thrombin cleavage, and removal of thrombin through benzamidine chromatography (GE Healthcare). Purity was further increased using Mono Q ion exchange chromatography. 1 mg ml^{-1} Ycf54 protein was used to generate rabbit polyclonal anti-Ycf54 antibody (Bio-Serv). Antibodies against *Synechocystis* MgP methyltransferase, PChlide oxidoreductase, and geranylgeranyl reductase were prepared using essentially the same protocol. An antibody against the *Synechocystis* ferrochelatase was kindly provided by Prof. Annegret Wilde (Justus-Liebig University, Giessen, Germany). The Sll1214 antibody (anti-Chl27) was obtained from Agrisera (Sweden).

Assessment of Gene Expression by Northern Blot and RT-PCR—WT and mutant cells were grown photomixotrophically at low light and harvested at an $OD_{750} \sim 0.4$. For Northern blot total RNA was purified according to Pinto *et al.* (25). 5 μg of purified RNA was than separated on 1.3% agarose formaldehyde gel and blotted onto Hybond-N^+ membrane (GE Healthcare). A hybridization probe was generated by random prime labeling (Rediprime II labeling kit, GE Healthcare) with [α-^{32}P]dCTP (Hartmann Analytic). The membrane was prehybridized for 60 min in 50% (v/v) deionized formamide, 7% SDS, 250 mM NaCl, and 120 mM sodium phosphate, pH 7.2, at 45 °C and hybridized overnight with a labeled probe. The membrane was than rinsed in 2× SSC, 1% SDS and washed in 2 subsequent 15-min steps at 48 °C in 2× SSC, 0.5% SDS and 0.1× SSC, 0.1% SDS, respectively. Signals were visualized using phosphorimaging. For RT-PCR 4×10^8 cells were disrupted by bead beating in the presence of RNAprotect (Qiagen). RNA was purified from the cell extract using the RNeasy kit (Qiagen) and RNase free DNase (Qiagen) according to the application manuals. cDNA was synthesized from 50 or 100 ng of RNA using SuperScript III Reverse Transcriptase (Invitrogen) and random primers (Invitrogen). RT-PCR was performed on cDNA using gene-specific primers, resolved on a 1% agarose gel, and visualized by ethidium bromide.

RESULTS

The Synechocystis Ycf54 Protein Forms a Complex with AcsF Homologs Sll1214 and Sll1874—To identify interacting partners/subunits of MgPME cyclase, we prepared *Synechocystis* strains expressing the AcsF homologs Sll1214 and Sll1874 as 3×FLAG-tagged proteins under control of the constitutive *psbAII* promoter. Western blotting with an anti-FLAG antibody showed that both tagged proteins were located exclusively in the membrane fraction (not shown). For pulldown assays, cells of both tagged strains were fractionated, and membrane fractions were solubilized by 1.5% dodecyl-β-maltoside and incubated with anti-FLAG affinity resin. After extensive washing with 100 column volumes of buffer, the FLAG-Sll1214 and FLAG-Sll1874 bait and prey proteins were eluted using the FLAG peptide. Fig. 1*A* shows SDS-electrophoresis analysis of elutions from FLAG pulldown assays; in both cases the FLAG-tagged Sll1214 or FLAG-Sll1874 proteins were the most prominent bands purified. Eluted proteins were derivatized by *S*-carbamidomethylation and digested by trypsin in the presence of SDS. The tryptic peptide fragments were prepared for MS analysis by solid phase extraction using a combination of cation exchange and C18 reversed-phase media. The peptides were subsequently analyzed using nano-LC/MS-MS in conjunction with ultra high resolution time of flight mass spectrometry enabling high mass accuracy in both the MS and tandem MS spectra.

Table 1 presents a list of the proteins identified using mass spectrometry analysis of the pulldown assays using either FLAG-Sll1214 or FLAG-Sll1874 as bait. Fig. 1, *B* and *C*, shows

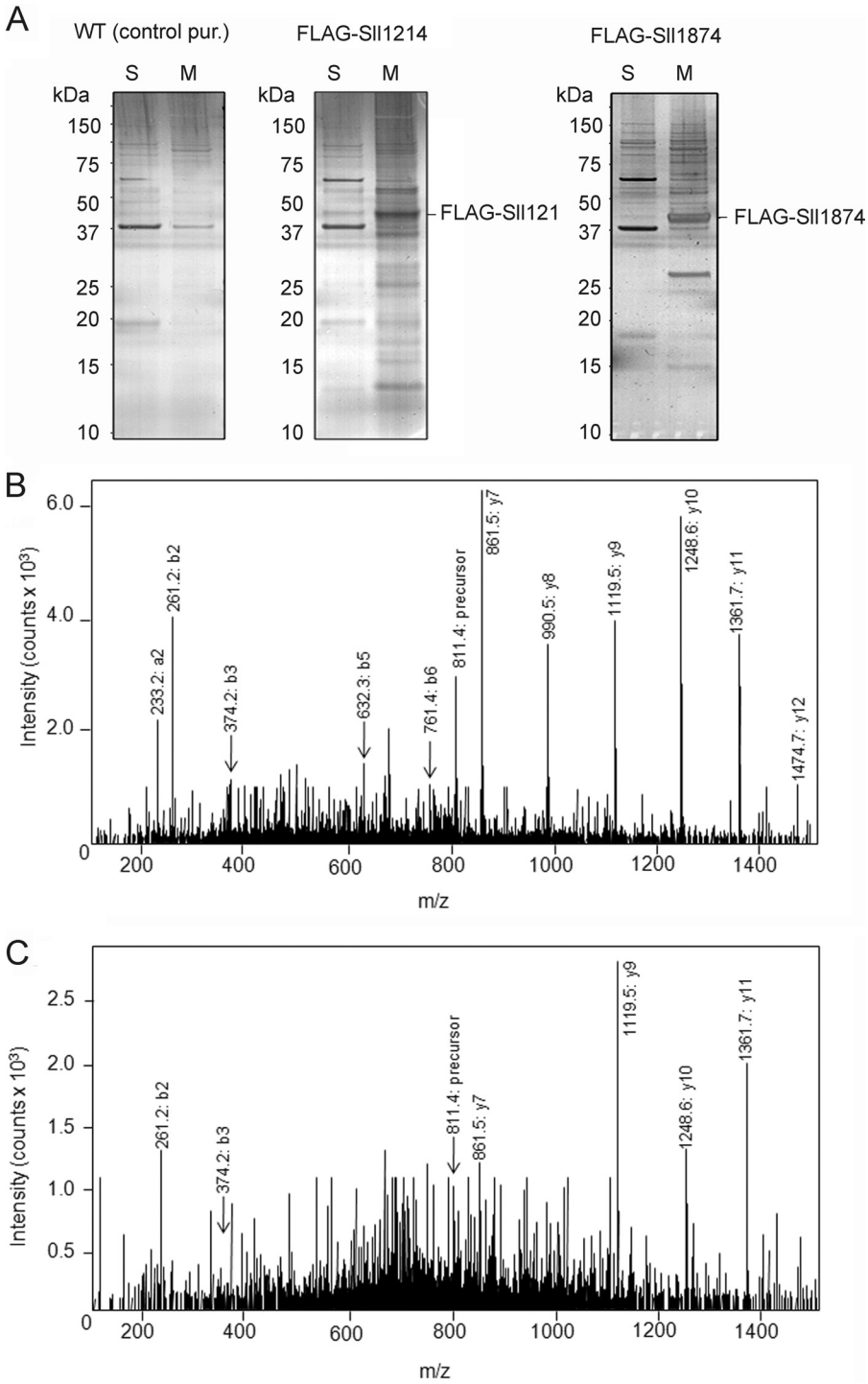

FIGURE 1. **Affinity purification of FLAG-Sll1214 and FLAG-Sll1874 and identification of Ycf54 by mass spectrometry.** *A*, FLAG-Sll1214 and FLAG-Sll1874 were purified from *Synechocystis* cytoplasmic (*S*) and dodecyl-β-maltoside-solubilized membrane (*M*) fractions using anti-FLAG agarose and eluted under native conditions with 3×FLAG peptide. Eluted proteins were resolved by SDS-PAGE and silver-stained; a WT eluate was used as a control. *B*, product ion (MS/MS) spectra of the proteotypic tryptic peptide FLLEEEPFEEVLK (*m/z* 811.4, 2+) for the Ycf54-like protein and from the FLAG-Sll1214 pulldown assay. This peptide was identified from database searches of the nano-LC-MS/MS data. *C*, procedures are were for *B*, but for the FLAG-Sll1874 pulldown.

product ion (MS/MS) spectra of the tryptic peptide FLLEEEP-FEEVLK (*m/z* 811.4, charge state 2+, mass 1620.8 Da) from the Ycf54-like protein from the FLAG-Sll1214 (Fig. 1*B*) and FLAG-Sll1874 (Fig. 1*C*) pulldown assays, respectively. These results show that using N-terminal FLAG-tagged Sll1214 and Sll1874 proteins as bait, each identifies Ycf54 as a potential interaction partner *in vivo*. Other proteins identified in both pulldown assays such as subunits of phycobilisomes and ATP synthase (Table 1) were presented also in the control WT sample (not shown), so these are regarded as false positives.

To lend further support to the proposed role of Ycf54 in the cyclase step of Chl biosynthesis, a construct encoding a FLAG-Ycf54 protein was expressed in the *Synechocystis* WT using the same methodology as described for FLAG-Sll1214/Sll1874, and

TABLE 1

Proteins identified by nano-LC-MS/MS and database searching in FLAG-Sll1214 and FLAG-Sll1874 pulldown assays

The tryptic peptides identified by database searching are shown with their neighboring residues in the sequence separated by periods.

Protein	Uniprot identifier gene name	Mass	Score	Coverage	Peptides
		Da		%	
Magnesium-protoporphyrin IX monomethyl ester oxidative cyclase Sll1214	P72584 ACSF1	42,525	783	29	R.YITIYR.H R.AILEEFR.V K.MDISPNEDELR.A K.MDISPNEDELR.A K.MDISPNEDELR.A R.FYTTDFDEMAK.M K.FIFYATYLSEK.I R.FYTTDFDEMAK.M R.ADFYACLGLEAR.S R.SCTAEFSGFLLYK.E R.AILEEFRVDYNR.H K.NKNPLLAECFNLMSR.D R.VFPIILDVNNPEFYNR.L R.FYTTDFDEMAKMDISPNEDELR.A
Allophycocyanin α chain	Q01951 PHAA	17,458	56	14	R.YLSPGELDR.I R.SLGTPIEAVAQSVR.E
Ycf54-like protein	P72777 YC54L	15,446	40	9	R.YLSPGELDR.I R.SLGTPIEAVAQSVR.E
	P26527 ATPB	51,758	23	3	K.FLLEEEPFEEVLKER.R
Magnesium-protoporphyrin IX monomethyl ester oxidative cyclase Sll1874	P74134 ACSF2	42,313	436	27	R.FYTTDFDK.V R.LAFIDFLER.S K.LAEAFHLLAR.D K.APVKETLLTPR.F R.TDFYQSVGLDAK.Q R.AFPEVLDTDNPK.F R.SCTSEFSGFLLFK.E R.AFPEVLDTDNPKFFPR.L K.VANLVLTLQDEEIEAALEELR.A
C-phycocyanin β chain	Q54714 PHCB	18,286	33	16	−.MFDVFTR.V R.GEYLSGSQLDALSATVAEGNKR.I
Ycf54-like protein	P72777 YC54L	15,446	26	11	K.FLLEEEPFEEVLK.E K.FLLEEEPFEEVLKER.R
Magnesium-protoporphyrin IX monomethyl ester oxidative cyclase Sll1214	P72584 ACSF1	42,525	25	8	R.AILEEFR.V R.ADFYACLGLEAR.S R.SCTAEFSGFLLYK.E
ATP synthase subunit α	P27179 ATPA	54,046	24	2	M.VSIRPDEISSIIR.Q
Allophycocyanin α chain	Q01951 PHAA	17,458	22	14	R.YLSPGELDR.I R.SLGTPIEAVAQSVR.E

another pulldown experiment was performed. As shown in Fig. 2*A*, FLAG-Ycf54 was successfully purified under native conditions, and analysis by SDS-PAGE shows a prominent silver-stained band. The FLAG-Ycf54 elution was then blotted and probed with anti-Chl27 antibody raised against the AcsF homologue from *Arabidopsis*. This antibody is known to be reactive to Sll1214, whereas reactivity to Sll1874 is minimal (20). Importantly, a clear signal from the Sll1214 cyclase component was detected (Fig. 2*B*), and subsequent MS analysis verified the presence of Sll1214 in the FLAG-Ycf54 eluate (not shown) but not in the control WT sample.

The ycf54 gene Is Required for Accumulation of Enzymes Catalyzing Several Steps of Chlorophyll Biosynthesis—To investigate the function of Ycf54, the cognate *sll1780* gene was inactivated by insertion of an erythromycin cassette. PCR analysis of genomic DNA confirmed the near-complete segregation of the mutant allele (supplemental Fig. 3*A*), but full segregation could not be achieved despite the various growth conditions tested combined with high concentrations of erythromycin (not shown). Nevertheless, the level of the *ycf54* transcript in the *ycf54* strain was clearly lowered (Fig. 3*A*), and a Western blot probed with the anti-Ycf54 antibody showed a significantly reduced level of Ycf54 compared with the WT strain (Fig. 3*C*). This antibody also allowed us to localize Ycf54 to both the soluble and membrane fractions (Fig. 3*C*). A lowered amount of Ycf54 was accompanied by a significant decrease in the level of Sll1214 and also in the amounts of the enzymes that precede and follow the cyclase step, MgP methyltransferase, and PChlide oxidoreductase. The level of geranylgeranyl reductase was also reduced to some extent. Interestingly, the level of MgP methyltransferase in the soluble fraction is similar in WT and mutant strains despite very different amounts bound to membranes. The association of MgP methyltransferase with the membrane is apparently weaker in the *ycf54* mutant or perhaps there is a specific degradation of this enzyme. In addition, we analyzed the level of ferrochelatase and found it comparable in the WT and the mutant, implying that the *ycf54* mutation specifically affects enzymes in Chl branch of the tetrapyrrole pathway (Fig. 3*C*).

To confirm that the observed changes in enzyme levels are not due to a positional effect of the *ycf54* mutation, the *ycf54* mutant was transformed by the FLAG-*ycf54* construct. Importantly, this complementation experiment made it possible to completely segregate the mutated *ycf54* gene (supplemental Fig. 3*B*). Fig. 3*C* shows that levels of all Chl biosynthesis enzymes examined were restored to WT levels in the complemented FLAG-*ycf54*/*ycf54*$^{-}$ strain. Thus, the reduction in the

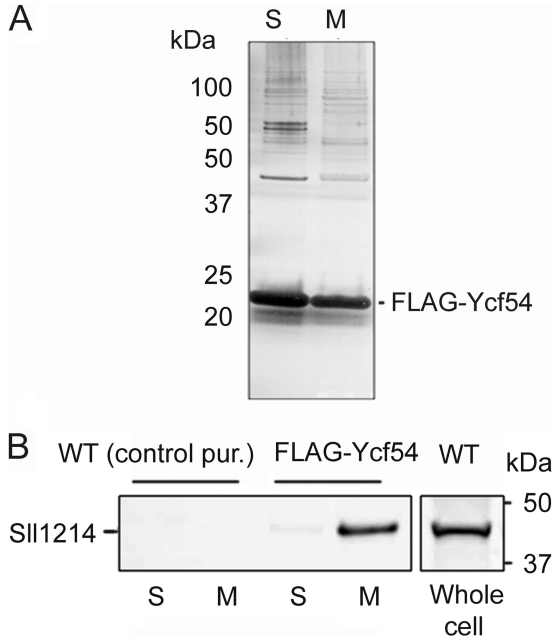

FIGURE 2. **Affinity purification of FLAG-Ycf54 and identification of Sll1214/Sll1874 by Western blot.** *A*, FLAG-Ycf54 was purified from a *Synechocystis* cytoplasmic fraction (*S*) and a dodecyl-β-maltoside-solubilized membrane fraction (*M*) using anti-FLAG-agarose and eluted with 3xFLAG peptide. Eluted proteins were resolved by SDS-PAGE and visualized with silver stain. *B*, Eluted proteins from the FLAG-Ycf54 pulldown assay were resolved by SDS-PAGE and transferred by Western blot to a nitrocellulose membrane. The amount of protein loaded for each sample corresponded to $^{1}/_{10}$ of the total eluate. The membrane was then probed with anti-Chl27 (Agrisera) raised against the AcsF homolog in *Arabidopsis*. The antibody is reactive to Sll1214 but not to Sll1874 (16). A WT control consisting of a *Synechocystis* whole cell lysate probed with anti-Chl27 is included for comparison.

levels of MgP methyltransferase and PChlide oxidoreductase in particular can be ascribed specifically to the *ycf54* mutation.

We further examined levels of transcripts for *sll1214* in the *ycf54* mutant, the WT, and in the complemented strain. Northern blotting shows that the level of the *sll1214* transcript is a bit reduced in the *ycf54* mutant, but no such decrease was observed in the complemented strain (Fig. 3*B*). A lowered level of the *sll1214* transcript in the mutant was detected also by RT-PCR, and a somewhat reduced expression was also found for the *por* gene (Fig. 3*A*).

Inactivation of the ycf54 Gene Impairs the Cyclase Step of Chlorophyll Biosynthesis—The phenotypic effects of inactivating the *sll1780* gene were investigated in cells grown under low light (3 μmol of photons m^{-2} s^{-1}) to minimize any effects of photo-oxidative damage arising from disrupted tetrapyrrole metabolism. To maintain the *ycf54* mutation, the growth medium was supplemented by 5 μg ml^{-1} of erythromycin; this level of antibiotic has no effect on a control WT strain harboring a genomic insertion of the erythromycin cassette in place of the *psbAII* gene (not shown). The *ycf54* cells obtained were markedly pale, suggesting a deficiency in photosynthetic pigments (see supplemental Fig. 3*C* for pictures of cultures of WT and *ycf54* strains). The Chl content per cell was reduced by 70% in the *ycf54* mutant relative to the WT (Fig. 4*A*). The complemented FLAG-*ycf54*/*ycf54*$^{-}$ strain has a much improved Chl content reaching almost 80% of the WT level (Fig. 4*A*), which is in line with the improved accumulation of enzymes in this strain (Fig. 3*C*). The appearance of an absorbance peak at 420 nm hints at the accumulation of a "new"' pigment produced by the *ycf54* mutation (Fig. 4*A*). To identify this component of the *ycf54* cell spectra, methanol extracts were prepared from equal quantities of *ycf54* and WT cells, then cellular pigments were separated and analyzed by HPLC. The *ycf54* chromatogram contains a distinct peak at 11 min that is completely absent in the WT sample (Fig. 4*B*). The elution time and absorbance and fluorescence spectra of this pigment identified it as MgPME (supplemental Fig. 4). Indeed, the 416-nm absorbance maximum of MgPME in solvent is consistent with the observed absorbance of *ycf54* cells at 420 nm.

The high content of MgPME in the *ycf54* mutant suggests that the pathway is specifically blocked at the cyclase step. To examine the effects of the *ycf54* mutation further, we quantified levels of Chl precursors and performed more detailed spectroscopic analyses. Methanol extracts from low light-grown cells were purified by phase partitioning, concentrated, and separated by HPLC. It should be noted that some P_{IX} is released by *ycf54* cells into the growth medium and that all such precipitated pigments were removed by filtration before cell extraction and HPLC analysis. Thus, the data in Fig. 5 reflect the intracellular accumulation of Chl biosynthetic intermediates. The fluorescence elution profiles for *ycf54* extracts in Fig. 5*A* show enhanced levels of P_{IX} (a 3.2-fold increase) and, as expected, a very high level of MgPME; this was quantified using the absorbance data in Fig. 5*B* as an ~100-fold increase. Use of the second fluorescence detector enabled quantification of MgP, which increased 4-fold in the mutant (results not shown). These large rises in Chl biosynthetic intermediates before the cyclase step in the pathway were accompanied by a dramatic decrease in the level of the product of the cyclase, PChlide, to 5% of the WT level. Interestingly, levels of Chlide are not altered significantly in the *ycf54* mutant in comparison with the WT (Fig. 5*A*), which suggests that this pool of Chlide results from Chl recycling rather than *de novo* synthesis (see "Discussion"). In summary, the accumulation of Chl precursors shows that although the *ycf54* mutation strongly decreases the amount of the MgP methyltransferase, there is no impairment of the pathway at this step, in contrast with the very low cyclase activity.

Further evidence for an essential role of Ycf54 in the cyclase step comes from inspection of the small elution peaks identified with an arrow in Fig. 5*A*, also identified as peaks at 7.6 and 8.0 min using detection of absorption (Fig. 5*B*). Fig. 6 shows a more detailed spectroscopic analysis of each elution component, neither of which corresponds to the product of the cyclase, PChlide, or of the cyclase substrate, MgPME (see the *inset* in Fig. 6). Instead, the Soret band at 432 nm, normalized to a value of 1.0 at this wavelength, is situated between that of MgPME at 416 nm and PChlide at 440 nm (see *inset* to Fig. 6*A*). Similar behavior is observed for the red-most bands, which are located at 614 nm for the 7.6-min component and 616-nm for the 8.0 min peak; the corresponding MgPME absorbance band is at 588 nm, and for PChlide the peak is at 630 nm. This pattern is also found in the fluorescence emission spectra in Fig. 6*B*, which clearly show the same progressive red shift, starting with MgPME at 595 nm, the two putative cyclase reaction intermediates at 620 and 628 nm, and ending with the cyclase product,

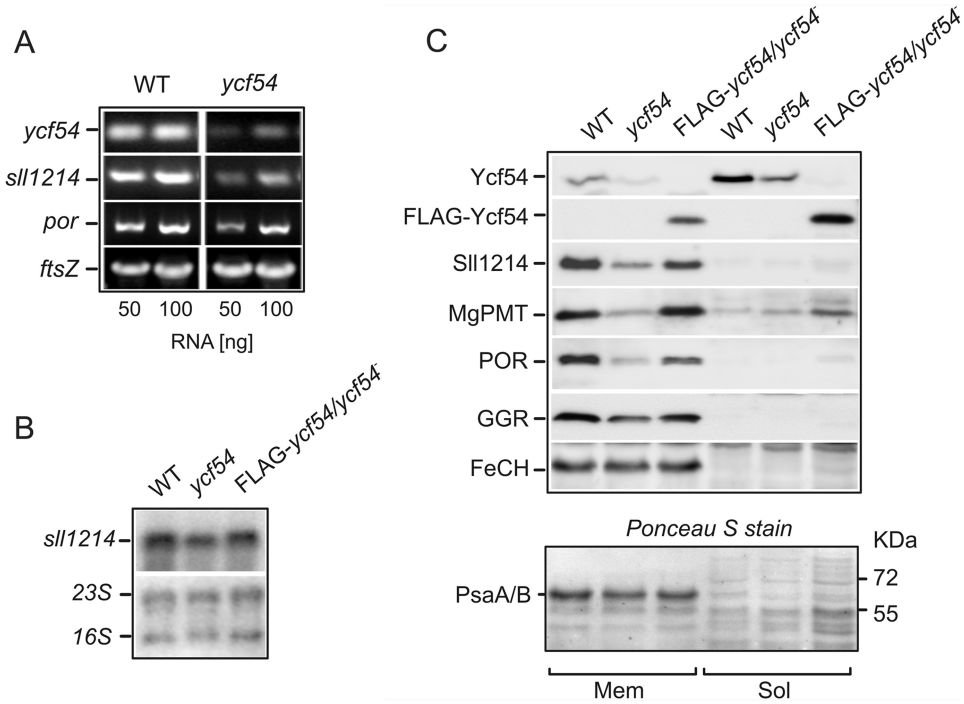

FIGURE 3. *A*, RT-PCR analysis of *ycf54*, *sll1214*, and *por* expression in the WT and *ycf54* mutant was performed using specific primers; the *ftsZ* transcript was included as a control. *B*, expression of the *sll1214* gene in the WT, *ycf54* mutant, and the FLAG-*ycf54*/*ycf54*$^-$ strain was analyzed using northern blotting. A DNA probe specific for *sll1214* was used for hybridization; RNA transcripts were used as a loading control. *C*, shown are levels and localization of Ycf54, FLAG-Ycf54, and enzymes of Chl biosynthesis in the WT, *ycf54* mutant, and the complemented FLAG-*ycf54*/*ycf54*$^-$ strain grown mixotrophically under low light conditions. The same amounts of protein of soluble (*Sol*) and membrane (*Mem*) fractions were separated by SDS-PAGE and blotted onto nitrocellulose. The membrane was probed using specific antibodies, which are listed on the *left-hand* side of the figure. The mobility of the FLAG-Ycf54 protein (*top row*) differs substantially from that of Ycf54, and the band for this protein is not shown. In the *second row*, the FLAG-Ycf54 protein was detected by the anti-FLAG antibody (Sigma). The *lower panel* shows blotted proteins stained with Ponceau S as a loading control. The band for the Photosystem I core PsaA/B subunits is indicated. The abbreviations used are: *MgPMT*, Mg-protoporphyrin methyltransferase; *POR*, protochlorophyllide oxidoreductase; *GGR*, geranylgeranyl reductase; *FeCH*, ferrochelatase.

PChlide, at 642 nm. On the basis of these spectra, it appears that *Synechocystis* cells harboring the *ycf54* mutation synthesize pigments with the absorption properties of possible cyclase reaction intermediates.

DISCUSSION

Based on available biochemical data and also with regard to the complexity of the enzymatic reaction required to create the fifth Chl ring (supplemental Fig. 1), the MgPME cyclase is expected to be active as a multisubunit complex. However, our knowledge of the individual components of this enzyme is very limited. In cucumber, barley, *C. reinhardtii*, and *Synechocystis* the MgPME cyclase was resolved into membrane and soluble components (6, 15, 26). In addition, the membrane component appears to be formed from at least two different proteins; the first one is a homolog of AcsF, and the second one is an as yet unknown protein deficient in the *viridis-k* mutant of barley (15). AcsF contains a putative diiron site and, thus, is viewed as a true catalytic subunit of MgPME cyclase (16).

Previous work had identified two genes in *Synechocystis*, *sll1214* and *sll1874,* as *acsF* homologs that encode the membrane component of the MgPME cyclase (20, 21). To identify their protein partners, we tagged the N termini of Sll1214 and Sll1874 *in vivo* with 3×FLAG and purified both proteins from detergent-solubilized membrane extracts. These experiments identified Ycf54 as a possible partner for Sll1214 and Sll1874. A reciprocal pulldown assay using FLAG-Ycf54 showed that Sll1214 is trapped as prey. The absence of Sll1874 in the FLAG-Ycf54 eluate is not so surprising bearing in mind the aerobic growth conditions used to prepare the culture of FLAG-*ycf54* strain; Sll1874 is specifically expressed under micro-oxic conditions, and its level is probably minimal under atmospheric oxygen level (20, 21). In contrast to the membrane-bound Sll1214/Sll1874, Ycf54 appears to be a rather hydrophilic protein (Fig. 3*C*); it is likely that the association of Ycf54 with membrane is provided via an interaction with AcsF homologs.

A partial inactivation of the *ycf54* gene produced a strong phenotype, greatly impeding cell growth and resulting in accumulation of Chl biosynthetic intermediates for the steps preceding the cyclase step in Chl biosynthesis. Given the essential nature of the cyclase step in the Chl biosynthetic pathway, it is perhaps not surprising that, despite repeated efforts, full segregation of the *ycf54* mutation could not be achieved. The importance of Ycf54 is underlined by the effects of the *ycf54* mutation, which include impaired accumulation of several enzymes of Chl biosynthesis including the AcsF homolog Sll1214 and significantly reduced Chl levels. This decrease in Sll1214 protein to the observed extent (Fig. 3*C*) would itself explain the observed 70% decrease in Chl in the *ycf54* mutant. The *sll1214*$^-$ *Synechocystis* mutant possessing about 50% of WT Sll1214 levels displays similar decreases in Chl content (21). In contrast, some other enzymes in tetrapyrrole biosynthesis appear to be present in apparent excess. For example, *Synechocystis* mutants

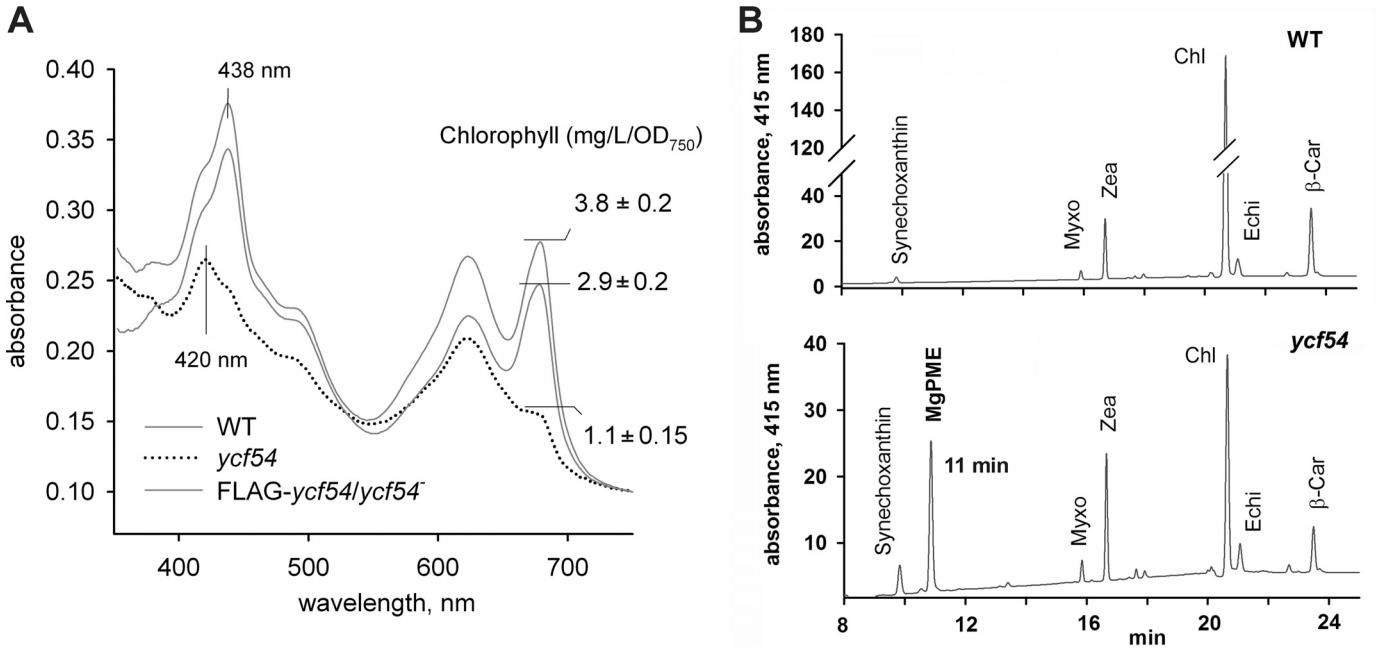

FIGURE 4. **Cell spectra and pigment content in the WT, *ycf54* mutant, and the complemented FLAG-*ycf54*/*ycf54*⁻ strain.** *A*, shown are absorbance spectra of *Synechocystis* whole cells grown mixotrophically under low light conditions. Chl *a* is represented by the 682-nm peak, and phycobiliproteins are represented by the 625-nm peak. Spectra were measured with cells in the logarithmic phase of growth (OD_{750} = ~ 0.3) and normalized to light scattering at 750 nm. *B*, shown is pigment content in the WT and *ycf54* strains grown mixotrophically under low light conditions. The same amount of cell material was extracted by methanol and separated by HPLC. The *ycf54* strain has a low Chl content but contains very high levels of the Chl precursor MgPME; this pigment is not detectable in methanol extracts of the WT (see also supplemental Fig. 4). *Myxo*, myxoxanthophyll; *Zea*, zeaxanthin; *Echi*, echinenon; *β-Car*, *β*-carotene.

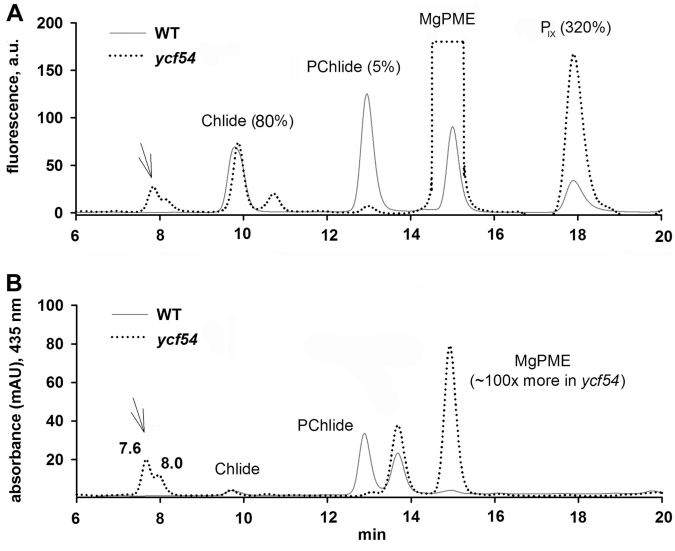

FIGURE 5. **Analysis of Chl precursors in the WT and *ycf54* strains grown mixotrophically under low light conditions.** Chl precursors were extracted with 80% methanol, 20% water, 0.2% NH_4OH from cells at OD_{750} = ~0.35 and analyzed by HPLC equipped with a diode array detector and a pair of fluorescence detectors (for detector settings see "Experimental Procedures"). *A*, shown is separation of precursors as detected by fluorescence detector 1; values indicate relative content of each precursor in the mutant when compared with WT. The concentration of MgPME in the *ycf54* strain exceeded the detection limit of the fluorescence detector. *B*, an identical run was recorded by the diode array detector at 435 nm. Two unusual pigments detected in the mutant at 7.6 and 8.0 min are also highlighted by an *arrow* (see Fig. 6 for absorbance spectra). The use of the diode array detector allowed an estimate of MgPME level that was approximately100 times higher in the *ycf54* strain relative to the WT. *a.u.*, absorbance units.

with 5–10% of WT levels of ferrochelatase are not deficient in heme and have no discernable phenotype (27, 24), whereas *Synechocystis* strains with reduced levels of Chl synthase have no growth or pigmentation defects.[6] This seems be also the case of MgP methyltransferase, where strongly reduced levels still produce plenty of MgPME in the *ycf54* mutant (Figs. 3*C* and 4*B*).

Although it appears that the level of Sll1214 is important for synthesis of PChlide and Ycf54 is essential for the accumulation of Sll1214, we cannot exclude the possibility that Ycf54 is directly involved in the catalytic function of the cyclase. Regarding the phenotype of the *ycf54* mutant together with our evidence showing that Ycf54 physically interacts with AcsF homologs, it is not unreasonable to consider Ycf54 as a new cyclase subunit. Given the presence of Ycf54 in the soluble cellular fraction, we do not expect that this protein is related to the *viridis-k* mutation that affects a membrane component (15). The elusive soluble component of MgPME cyclase was reported to have a mass above 30 KDa (26), which is apparently at odds with the 12.5 KDa mass of Ycf54. In relation to a catalytic role, the structure of Ycf54 from *Thermosynechococcus elongatus* (PDB code 3HZE, see supplemental Fig. S5) shows that this protein does not contain any apparent redox or electron transfer sites that would support its role in catalysis. Taking into account the very low accumulation of Sll1214 in the *ycf54* mutant, it looks more probable that Ycf54 plays a critical role in AcsF synthesis/maturation or in the process of cyclase assembly rather than being a subunit of the cyclase enzyme complex.

There is, however, another possibility that Ycf54 facilitates formation of a catalytic complex between cyclase and preceding or after enzymes, and this interaction is required for cyclase

[6] R. Sobotka, unpublished data.

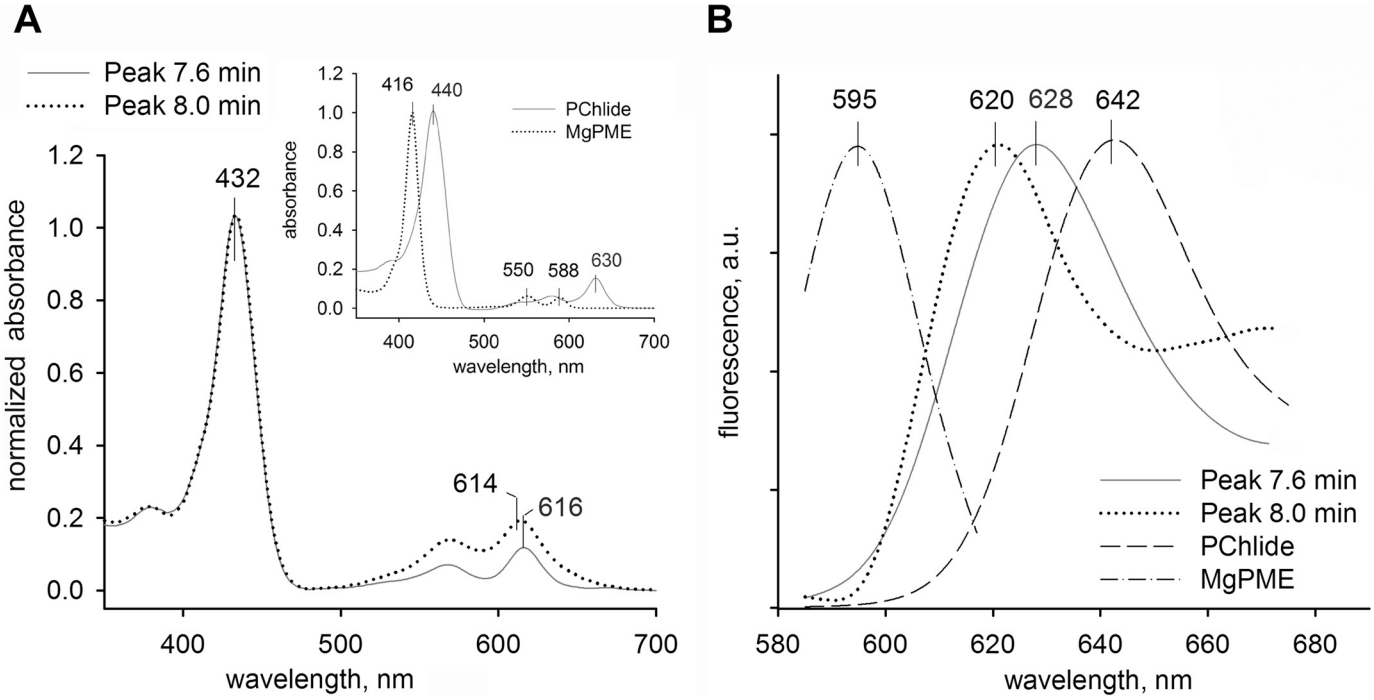

FIGURE 6. **Absorbance and fluorescence spectra of two unusual pigments found in the *ycf54* strain.** *A*, shown are absorbance spectra recorded by HPLC diode array detector. Pigments are described according to the time of elution from the HPLC column (7.6 and 8 min; see Fig. 5) and normalized to an absorbance at 432 nm = 1. The *inset* shows absorbance spectra of MgPME and PChlide obtained using the same detector. *B*, shown are fluorescence emission spectra recorded by the HPLC fluorescence detector and normalized to the same maximum of fluorescence. The 7.6- and 8.0-min peaks and PChlide were excited at 435 nm; MgPME was excited at 416 nm.

activity. The Chl intermediates that accumulate in the *ycf54* mutant, P_{IX}, MgP, and MgPME, all precede the cyclase step in the Chl biosynthetic pathway. If the enzymes for the first three steps of the Chl pathway all act independently of each other, one might expect that the rise in pigment levels would be confined to just MgPME, the substrate for the cyclase. The observed increase in pigments all the way back to P_{IX}, the "branch point" substrate for both Mg-chelatase and ferrochelatase, argues for some coupling between the Mg-chelatase, MgP methyltransferase, and cyclase steps, so that the effects of MgPME accumulation are transmitted back along the pathway. Indeed, mechanistic coupling between the Mg-chelatase and methyltransferase steps has been demonstrated (28). Disrupted channeling of intermediates between MgP methyltransferase and the cyclase by a deficiency in Ycf54 could impair the stability of enzymes along the Chl pathway. Inactivation of the cyclase in tobacco has already been observed to have a negative effect on the level of PChlide oxidoreductase (29). We observed lowered levels of *sll1214* and *por* transcripts (Fig. 3, *A* and *B*), so it appears that the proposed assembly of a catalytic complex could involve coupled transcription, translation, and protein folding.

Interestingly, the structure of Ycf54 exhibits a similarity with the structure of the Psb28 protein (see supplemental Fig. 5). Deletion of the gene encoding Psb28 also affects PChlide synthesis in *Synechocystis* (30), although not to the extent observed in the *ycf54* mutant. Given that Psb28 binds CP47 during the process of photosystem II assembly (30), this protein might be a good candidate for a factor harmonizing Chl biosynthesis and photosystem II biogenesis.

There is a sharp contrast between the large decrease in PChlide and the unaffected level of Chlide. It might be expected that the demands of assembling photosynthetic complexes in a mutant that can synthesize only 5% of the normal amount of PChlide would exhaust the Chlide pool. This precursor is, however, also an intermediate in the constant process of recycling Chl (31), which might be accelerated in the *ycf54* mutant, resulting in replenished levels of Chlide. The fact that an apparently unaffected Chlide level can exist in a cell severely depleted in photosynthetic complexes suggests the existence of two separate Chlide pools, one filled by PChlide reductases and destined for *de novo* synthesis of photosystems and the other arising from de-phytolation of Chls. It seems that *de novo* production of Chl is essential to build new photosystems despite the existence of a pool of Chlide that probably originates from recycled Chl. It is also possible that there is a pool of Chlide-binding proteins that releases the pigment only when more Chlide is supplied by *de novo* production.

Analysis of the absorption and fluorescence emission spectra (Fig. 6) revealed some intriguing spectroscopic properties for the 7.6- and 8-min elution peaks identified in Fig. 5, *A* and *B*. The absorbance features of these pigments extracted from the *ycf54* mutant resemble those found in earlier work when greening cucumber cotyledons from etiolated plants were studied using fluorometry (32). In these experiments, MgPME-enriched cotyledons were illuminated for 5 h, and emission features were observed at ~596, ~603, and at 614–617 nm, with 420-nm excitation. The excitation spectra for these various emission peaks had a single maximum, at 434–436 nm (32), that matches well with the 432-nm absorbance maximum of a

pigment (Fig. 6*A*) produced by the *ycf54* mutant. These pigments, called "longer wavelength metalloporphyrins," were proposed as biosynthetic intermediates between MgPME and PChlide (32). However, the unusual pigments we observed in the *ycf54* strain and probably also the pigments identified in (32) do not correspond to the chemically synthesized cyclase intermediates used by Wong *et al.* (8); the spectroscopic properties of 6-methyl-β-hydroxy-MgPME are very similar to those of MgPME (33), and the 6-methyl-β-keto derivative has a similar absorbance spectrum red-shifted by just a few nanometers (34). Early studies of the cyclase employed enzyme assays based on fractionated extracts prepared from chloroplasts and could not benefit from current methods using the recombinant production of proteins. The lack of any mechanistic data on the MgPME cyclase is in sharp contrast to recent progress in the kinetic analysis of other enzymes in the Chl biosynthetic pathway, for example with Mg chelatase, MgP methyltransferase, and PChlide oxidoreductase (35–37). The identification of Ycf54 as a factor critical for the activity of MgPME cyclase *in vivo* should allow further progress with the biochemical analysis of this step in chlorophyll biosynthesis.

REFERENCES

1. Tanaka, R., and Tanaka, A. (2007) Tetrapyrrole biosynthesis in higher plants. *Annu. Rev. Plant Biol.* **58,** 321–346
2. Chereskin, B. M., Wong, Y. S., and Castelfranco, P. A. (1982) *In vitro* synthesis of the chlorophyll isocyclic ring. Transformation of magnesium-protoporphyrin IX and magnesium-protoporphyrin IX monomethyl ester into magnesium-2,4-divinyl pheoporphyrin A(5). *Plant Physiol.* **70,** 987–993
3. Fuesler, T. P., Wong, Y. S., and Castelfranco, P. A. (1984) Localization of Mg-chelatase and Mg-protoporphyrin IX monomethyl ester (oxidative) cyclase activities within isolated, developing cucumber chloroplasts. *Plant Physiol.* **75,** 662–664
4. Wong, Y. S., and Castelfranco, P. A. (1984) Resolution and reconstitution of Mg-protoporphyrin IX monomethyl ester (oxidative) cyclase, the enzyme system responsible for the formation of the chlorophyll isocyclic ring. *Plant Physiol.* **75,** 658–661
5. Nasrulhaq-Boyce, A., Griffiths, W. T., and Jones, O. T. (1987) The use of continuous assays to characterize the oxidative cyclase that synthesizes the chlorophyll isocyclic ring. *Biochem. J.* **243,** 23–29
6. Bollivar, D. W., and Beale, S. I. (1996) The chlorophyll biosynthetic enzyme Mg-protoporphyrin IX monomethyl ester (oxidative) cyclase. Characterization and partial purification from *Chlamydomonas reinhardtii* and *Synechocystis* sp. PCC 6803. *Plant Physiol.* **112,** 105–114
7. Granick, S. (1948) The structural and functional relationships between heme and chlorophyll. *Harvey Lect.* **44,** 220–245
8. Wong, Y. S., Castelfranco, P. A., Goff, D. A., and Smith, K. M. (1985) Intermediates in the formation of the chlorophyll isocyclic ring. *Plant Physiol.* **79,** 725–729
9. Walker, C. J., Mansfield, K. E., Smith, K. M., and Castelfranco P. A. (1989) Incorporation of atmospheric oxygen into the carbonyl functionality of the protochlorophyllide isocyclic ring. *Biochem. J.* **257,** 599–602
10. Taylor, D. P., Cohen, S. N., Clark, W. G., and Marrs, B. L. (1983) Alignment of genetic and restriction maps of the photosynthesis region of the *Rhodopseudomonas capsulata* chromosome by a conjugation-mediated marker rescue technique. *J. Bacteriol.* **154,** 580–590
11. Hunter, C. N., and Coomber, S. A. (1988) Cloning and oxygen-regulated expression of the bacteriochlorophyll biosynthesis genes *bchE*, *bchB*, *bchA*, and *bchC* of *Rhodobacter sphaeroides*. *J. Gen. Microbiol.* **134,** 1491–1497
12. Coomber, S. A., Chaudhri, M., Connor, A., Britton, G., and Hunter, C. N. (1990) Localized transposon Tn5 mutagenesis of the photosynthetic gene cluster of *Rhodobacter sphaeroides*. *Mol. Microbiol.* **4,** 977–989
13. Porra, R. J., Schäfer, W., Katheder, I., and Scheer, H. (1995) The derivation of the oxygen atoms of the 13(1)-oxo and 3-acetyl groups of bacteriochlorophyll *a* from water in *Rhodobacter sphaeroides* cells adapting from respiratory to photosynthetic conditions. Evidence for an anaerobic pathway for the formation of isocyclic ring E. *FEBS Lett.* **371,** 21–24
14. Porra, R. J., Schäfer, W., Gad'on, N., Katheder, I., Drews, G., and Scheer, H. (2004) Origin of the two carbonyl oxygens of bacteriochlorophyll *a*. Demonstration of two different pathways for the formation of ring E in *Rhodobacter sphaeroides* and *Roseobacter denitrificans* and a common hydratase mechanism for 3-acetyl group formation. *FEBS J.* **239,** 85–92
15. Rzeznicka, K., Walker, C. J., Westergren, T., Kannangara, C. G., von Wettstein, D., Merchant, S., Gough, S. P., and Hansson, M. (2005) Xantha-l encodes a membrane subunit of the aerobic Mg-protoporphyrin IX monomethyl ester cyclase involved in chlorophyll biosynthesis. *Proc. Natl. Acad. Sci.* **102,** 5886–5891
16. Pinta, V., Picaud, M., Reiss-Husson, F., and Astier, C. (2002) *Rubrivivax gelatinosus* acsF (previously orf358) codes for a conserved, putative binuclear-iron-cluster-containing protein involved in aerobic oxidative cyclization of Mg-protoporphyrin IX monomethylester. *J. Bacteriol.* **184,** 746–753
17. Ouchane, S., Steunou, A. S., Picaud, M., and Astier, C. (2004) Aerobic and anaerobic Mg-protoporphyrin monomethyl ester cyclases in purple bacteria. A strategy adopted to bypass the repressive oxygen control system. *J. Biol. Chem.* **279,** 6385–6394
18. Moseley, J. L., Page, M. D., Alder, N. P., Eriksson, M., Quinn, J., Soto, F., Theg, S. M., Hippler, M., and Merchant, S. (2002) Reciprocal expression of two candidate di-iron enzymes affecting photosystem I and light-harvesting complex accumulation. *Plant Cell* **14,** 673–688
19. Tottey, S., Block, M. A., Allen, M., Westergren, T., Albrieux, C., Scheller, H. V., Merchant, S., and Jensen, P. E. (2003) *Arabidopsis* CHL27, located in both envelope and thylakoid membranes, is required for the synthesis of protochlorophyllide. *Proc. Natl. Acad. Sci. U.S.A.* **100,** 16119–16124
20. Minamizaki, K., Mizoguchi, T., Goto, T., Tamiaki, H., and Fujita, Y. (2008) Identification of two homologous genes, chlAI and chlAII, that are differentially involved in isocyclic ring formation of chlorophyll *a* in the cyanobacterium *Synechocystis* sp. PCC 6803. *J. Biol. Chem.* **283,** 2684–2692
21. Peter, E., Salinas, A., Wallner, T., Jeske, D., Dienst, D., Wilde, A., and Grimm, B. (2009) Differential requirement of two homologous proteins encoded by sll1214 and sll1874 for the reaction of Mg protoporphyrin monomethylester oxidative cyclase under aerobic and micro-oxic growth conditions. *Biochim. Biophys. Acta* **1787,** 1458–1467
22. Rippka, R., Deruelles, J., Waterbury, J. B., Herdman, M., and Stanier, R. Y. (1979) Generic assignments, strain histories and properties of pure cultures of cyanobacteria. *J. Gen. Microbiol.* **111,** 1–61
23. Porra, R. J., Thompson,W. A., and Kriedemann, P. E. (1989) Determination of accurate extinction coefficients and simultaneous equations for assaying chlorophylls *a* and *b* extracted with four different solvents. Verification of the concentration of chlorophyll standards by atomic absorption spectroscopy. *Biochim. Biophys. Acta* **975,** 384–394
24. Sobotka, R., Tichy, M., Wilde, A., and Hunter, C. N. (2011) Functional assignments for the carboxyl-terminal domains of the ferrochelatase from *Synechocystis* PCC 6803. The CAB domain plays a regulatory role, and region II is essential for catalysis. *Plant Physiol.* **155,** 1735–1747
25. Pinto, F. L., Thapper, A., Sontheim, W., and Lindblad, P. (2009) Analysis of current and alternative phenol based RNA extraction methodologies for cyanobacteria. *BMC Mol. Biol.* **10,** 79
26. Walker, C. J., Castelfranco, P. A., and Whyte, B. J. (1991) Synthesis of divinyl protochlorophyllide. Enzymological properties of the Mg-protoporphyrin IX monomethyl ester oxidative cyclase system. *Biochem. J.* **15,** 691–697
27. Sobotka, R., Komenda, J., Bumba, L., and Tichy, M. (2005) Photosystem II assembly in CP47 mutant of *Synechocystis* sp. PCC 6803 is dependent on the level of chlorophyll precursors regulated by ferrochelatase. *J. Biol. Chem.* **280,** 31595–31602
28. Shepherd, M., McLean, S., and Hunter, C. N. (2005) Kinetic basis for linking the first two enzymes of chlorophyll biosynthesis. *FEBS J.* **272,** 4532–4539
29. Peter, E., Rothbart, M., Oelze, M. L., Shalygo, N., Dietz, K. J., Grimm, B.

(2010) Mg protoporphyrin monomethylester cyclase deficiency and effects on tetrapyrrole metabolism in different light conditions. *Plant Cell Physiol.* **51,** 1229–1241
30. Dobáková, M., Sobotka, R., Tichý, M., and Komenda, J. (2009) Psb28 protein is involved in the biogenesis of the photosystem II inner antenna CP47 (PsbB) in the cyanobacterium *Synechocystis* sp. PCC 6803. *Plant Physiol.* **149,** 1076–1086
31. Vavilin, D., and Vermaas, W. F. (2007) Continuous chlorophyll degradation accompanied by chlorophyllide and phytol reutilization for chlorophyll synthesis in *Synechocystis* sp. PCC 6803. *Biochim. Biophys. Acta* **7,** 920–929
32. Rebeiz, C. A., Mattheis, J. R., Smith, B. B., Rebeiz, C., and Dayton, D. F. (1975) Chloroplast Biogenesis. Biosynthesis and accumulation of Mg-protoporphyrin IX monoester and longer wavelength metalloporphyrins by greening cotyledons. *Arch Biochem. Biophys* **166,** 446–465
33. Walker, C. J., Mansfield, K. E., Rezzano, I. N., Hanamoto, C. M., Smith, K. M., and Castelfranco, P. A. (1988) The magnesium-protoporphyrin IX (oxidative) cyclase system. Studies on the mechanism and specificity of the reaction sequence. *Biochem. J.* **15,** 685–692
34. Smith, K. M., and Goff, D. A. (1986) Syntheses of some proposed biosynthetic precursors to the isocyclic ring in chlorophyll *a. J. Org. Chem.* **51,** 657–666
35. Viney, J., Davison, P. A., Hunter, C. N., and Reid, J. D. (2007) Direct measurement of metal-ion chelation in the active site of the AAA+ ATPase magnesium chelatase. *Biochemistry* **46,** 12788–12794
36. McLean, S., and Hunter, C. N. (2009) An enzyme-coupled continuous spectrophotometric assay for magnesium protoporphyrin IX methyltransferases. *Anal. Biochem.* **394,** 223–228
37. Heyes, D. J., and Hunter, C. N. (2005) Making light work of enzyme catalysis. Protochlorophyllide oxidoreductase. *Trends Biochem. Sci.* **30,** 642–649

SUPPLEMENTARY FIGURES

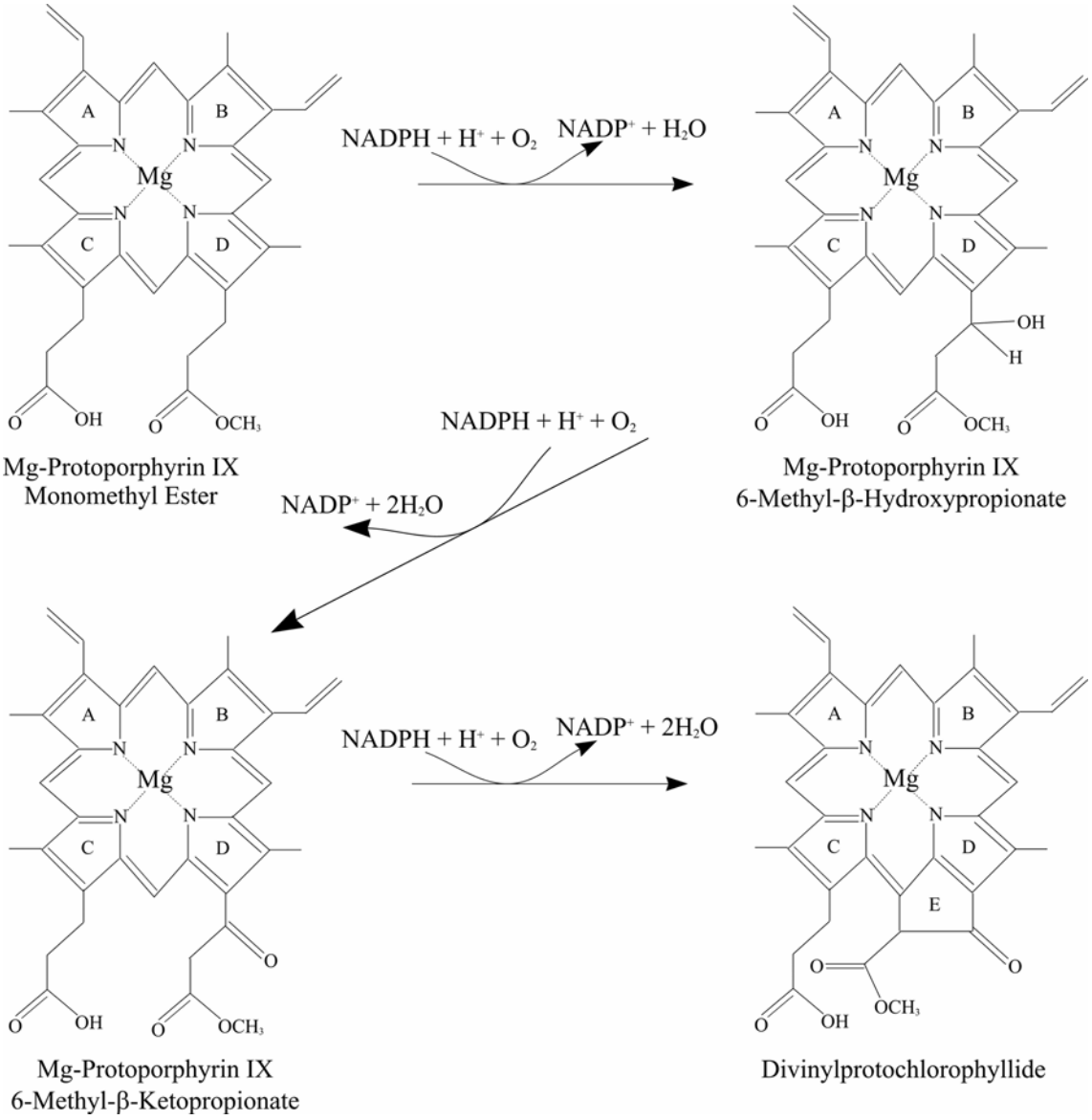

FIGURE S1. The oxidative cyclase reaction for the formation of the fifth ring of the Chl *a* molecule. In the proposed model the conversion of MgPME to divinyl protochlorophyllide proceeds through three sequential two-electron oxidations.

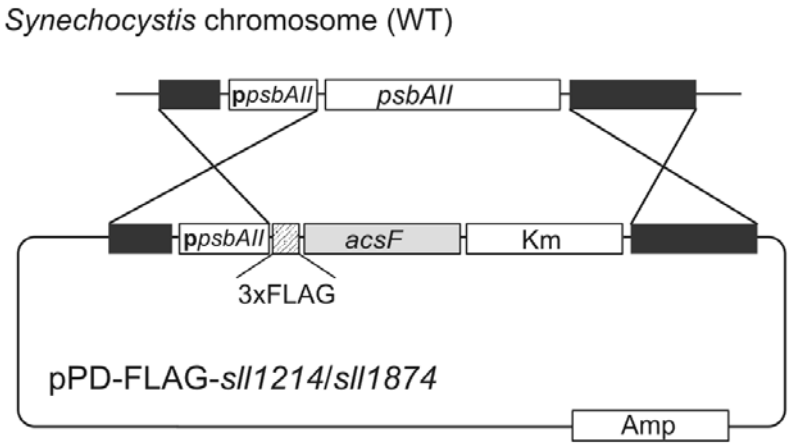

FIGURE S2. Preparation of the FLAG-Sll1214/Sll1874 strains using the pPD-FLAG plasmid. The *acsF* homolog genes were first cloned into the pPD-FLAG plasmid containing the 3xFLAG tag, the *Synechocystis psbAII* promoter and up- and down-stream sequences, which promote homologous recombination between the plasmid and the *Synechocystis psbAII* gene. Following transformation into *Synechocystis* WT the 3xFLAG-*sll1214/sll1874* genes were incorporated into the chromosome replacing the original *psbAII* gene; transformants were selected by resistance to neomycin.

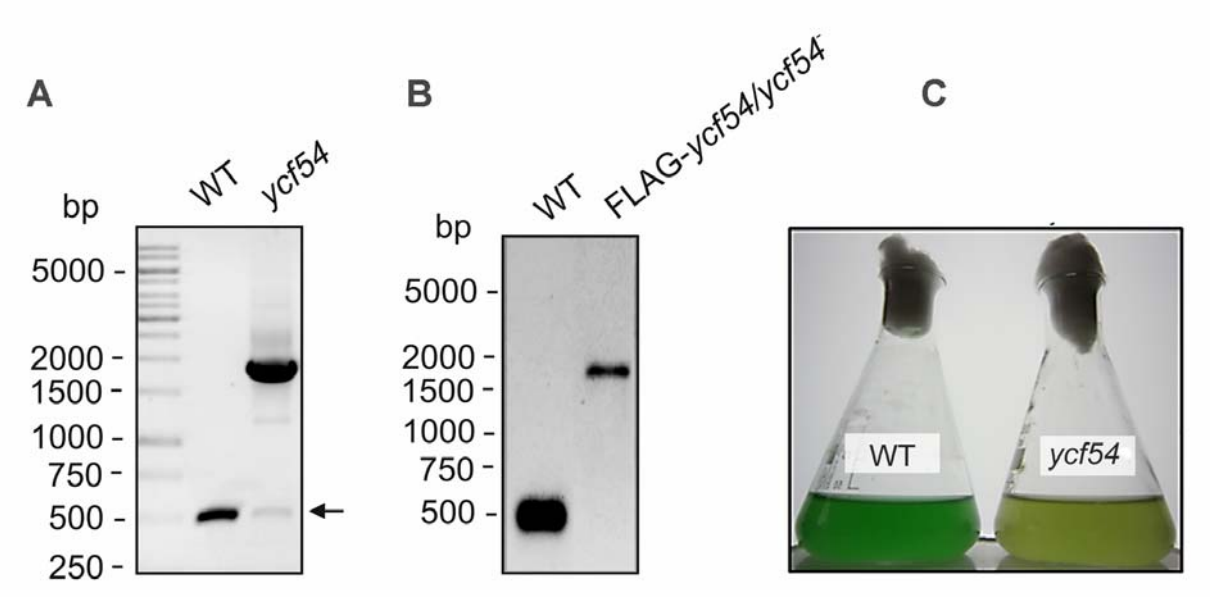

FIGURE S3. A, PCR analysis of the *ycf54* gene using DNA from the WT and the *ycf54* mutant as templates. The mutant *ycf54* copy gave rise to a larger PCR fragment of 1.8 kilobase pairs due to the insertion of the erythromycin resistance cassette (1.3 kilobase pairs). The arrow marks a faint band of ~500 bp indicating incomplete segregation of the mutated gene. **B**, Essentially the same PCR analysis using DNA from the WT and the complemented FLAG-*ycf54*/*ycf54*$^{-}$ strain. **C,** Visual comparison of WT and *ycf54* cultures grown photomixotrophically under low light conditions to a cell density of OD_{750} = 0.45. Culture of the *ycf54* mutant exhibits a pale yellowish colour.

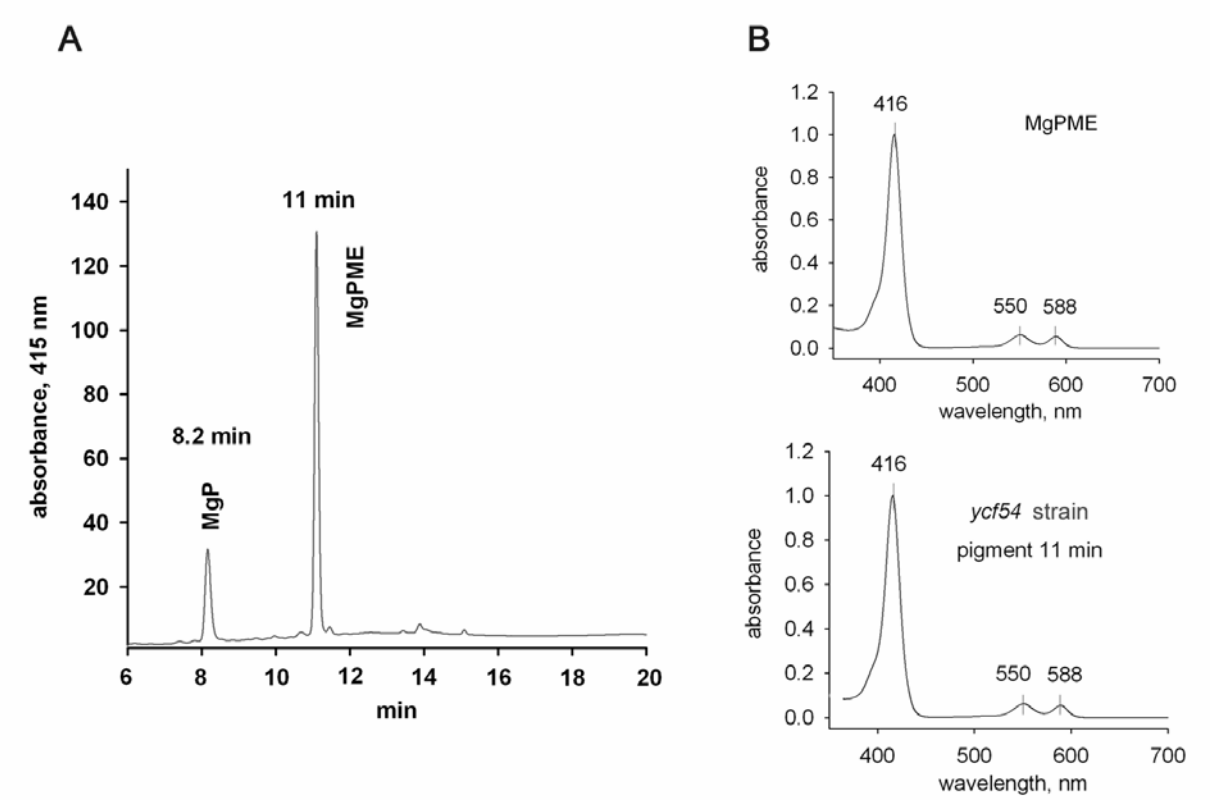

FIGURE S4. **A,** A control HPLC of MgP and MgPME standards separated by using the same conditions as described in Fig. 4B. Both pigments are clearly distinguished by elution time and that of MgPME (11 min) corresponds to the pigment accumulating in the *ycf54* mutant (see Fig. 4B). Chemical standards of MgP and MgPME were obtained from Frontier Scientific (USA). **B,** Absorption spectra of MgPME compared with the spectra of pigment accumulating in the *ycf54* mutant and eluted at 11 min; fluorescence emission spectra of these two compounds are also identical with maximum at 595 nm (not shown).

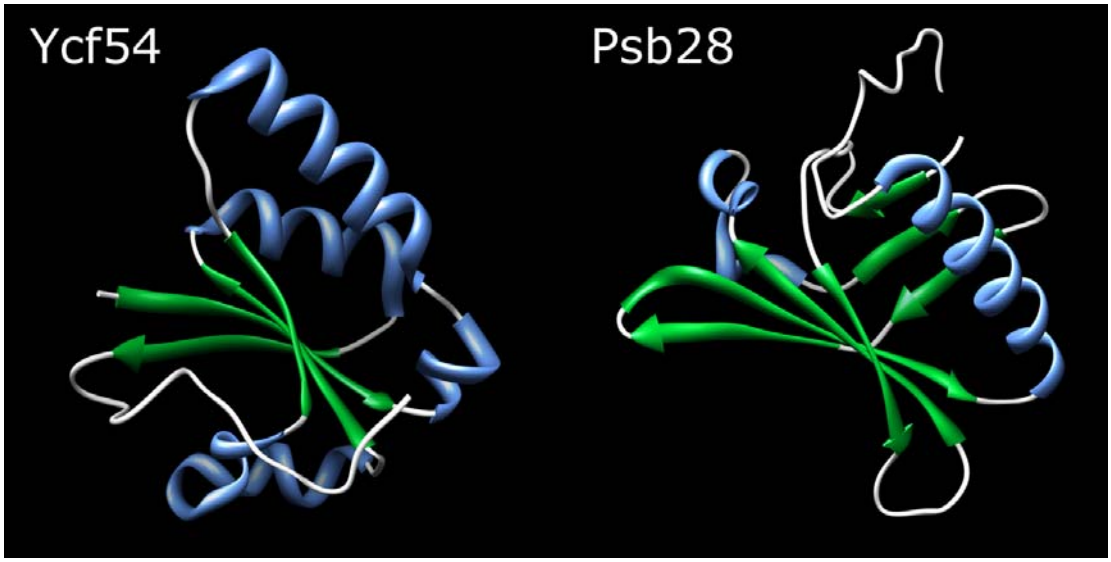

FIGURE S5. Crystal structures of Ycf54 from *Thermosynechococcus elongatus* (PDB code 3HZE, 1) and Psb28 from *Synechocystis* 6803 (PDB code 2KVO, 2).

1. Kuzin, A., Abashidze, M., Seetharaman, J., Sahdev, S., Xiao, R., Ciccosanti, C., Lee, D., Everett, J.K., Nair, R., Acton, T.B., Rost, B., Montelione, G.T., Hunt, J.F., Tong, L. Not published.

2. Yang, Y., Ramelot, T.A., Cort, J.R., Wang, D., Ciccosanti, C., Hamilton, K., Nair, R., Rost, B., Acton, T.B., Xiao, R., Everett, J.K., Montelione, G.T., and Kennedy, M.A. (2011) Solution NMR structure of photosystem II reaction center protein Psb28 from *Synechocystis* sp. Strain PCC 6803. *Proteins* **79**, 340-344

Conserved Chloroplast Open-reading Frame *ycf54* Is Required for Activity of the Magnesium Protoporphyrin Monomethylester Oxidative Cyclase in *Synechocystis* PCC 6803

Sarah Hollingshead, Jana Kopecná, Philip J. Jackson, Daniel P. Canniffe, Paul A. Davison, Mark J. Dickman, Roman Sobotka and C. Neil Hunter

J. Biol. Chem. 2012, 287:27823-27833.
doi: 10.1074/jbc.M112.352526 originally published online June 18, 2012